

CONF-900772-5

LBL-29488



# Lawrence Berkeley Laboratory

UNIVERSITY OF CALIFORNIA

Presented at the Workshop on Experiments and Detectors for RHIC, Upton, NY, July 2-7, 1988, and to be published in the Proceedings

Rec'd by STI

OCT 0 4 1990

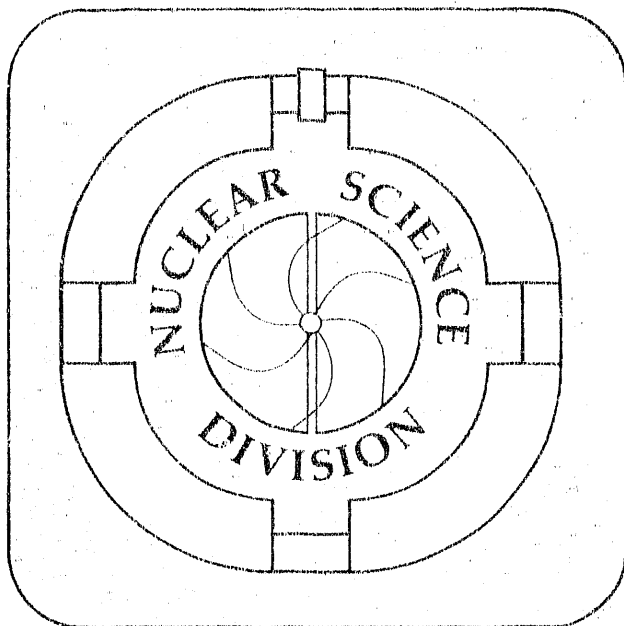
## Concept for an Experiment on Particle and Jet Production at Midrapidity

LBL-29488

J.W. Harris et al.

DE91 000190

July 1990



DISTRIBUTION OF THIS DOCUMENT IS UNLIMITED

Prepared for the U.S. Department of Energy under Contract Number DE-AC03-76SF00098.

## Concept for an Experiment on Particle and Jet Production at Midrapidity

J.W. Harris,<sup>7</sup> M. Bloomer,<sup>7</sup> P. Brady,<sup>1</sup> J. Carroll,<sup>2</sup> S.I. Chase,<sup>7</sup> W. Christie,<sup>7</sup>  
 J. Cramer,<sup>12</sup> E. Friedlander,<sup>7</sup> D. Greiner,<sup>7</sup> C. Gruhn,<sup>7</sup> M. Gyulassy,<sup>7</sup> T. Hallman,<sup>4</sup>  
 E. Hjort,<sup>10</sup> G. Igo,<sup>2</sup> P. Jacobs,<sup>7</sup> K. Kadija,<sup>13</sup> D. Keane,<sup>5</sup> L. Madansky,<sup>4</sup> C. Naudet,<sup>7</sup>  
 D. Nygren,<sup>7</sup> G. Odyniec,<sup>7</sup> D. Olson,<sup>7</sup> G. Paic,<sup>13</sup> A. Poskanzer,<sup>7</sup> G. Rai,<sup>7</sup> H.G. Ritter,<sup>7</sup>  
 R. Scharenberg,<sup>10</sup> L.S. Schroeder,<sup>7</sup> P. Seidl,<sup>7</sup> P. Seyboth,<sup>8</sup> D. Shy,<sup>7</sup> R. Stock,<sup>3</sup>  
 T.J. M. Symons,<sup>7</sup> L. Teitelbaum,<sup>7</sup> M.L. Tincknell,<sup>9</sup> H. van Hecke,<sup>6</sup> X.N. Wang,<sup>7</sup>  
 R. Welsh,<sup>4</sup> W. Wenzel,<sup>7</sup> H. Wieman,<sup>7</sup> and K.L. Wolf<sup>11</sup>

This work was supported in part by the Director, Office of Energy Research, division of Nuclear Physics of the Office of High Energy and Nuclear Physics of the U.S. Department of Energy under contract DE-AC03-76SF00098.

- 
- 1 University of California, Davis, California 95616, U.S.A.
  - 2 University of California, Los Angeles California 90024, U.S.A.
  - 3 University of Frankfurt, D-5000 Frankfurt am Main 90, West Germany.
  - 4 The Johns Hopkins University, Baltimore, Maryland 21218, U.S.A.
  - 5 Kent State University, Kent Ohio 44242, U.S.A.
  - 6 Los Alamos National Laboratory, Los Alamos, New Mexico, U.S.A.
  - 7 Lawrence Berkeley Laboratory, Berkeley, California 94720, U.S.A.
  - 8 Max Planck Institute for Physics, Munich, West Germany
  - 9 Oak Ridge National Laboratory, Oak Ridge, Tennessee, U.S.A.
  - 10 Purdue University, West Lafayette, Indiana 47907, U.S.A.
  - 11 Texas A&M University, College Station, Texas 77843, U.S.A.
  - 12 University of Washington, Seattle, Washington 98195, U.S.A.
  - 13 Rudjer Boskovic Institute, 41001 Zagreb, Yugoslavia

**MASTER** *DMS*

DISTRIBUTION OF THIS DOCUMENT IS UNLIMITED

## Concept for an Experiment on Particle and Jet Production at Midrapidity\*

J.W. Harris,<sup>7</sup> M. Bloomer,<sup>7</sup> P. Brady,<sup>1</sup> J. Carroll,<sup>2</sup> S.I. Chase,<sup>7</sup> W. Christie,<sup>7</sup>  
J. Cramer,<sup>12</sup> E. Friedlander,<sup>7</sup> D. Greiner,<sup>7</sup> C. Gruhn,<sup>7</sup> M. Gyulassy,<sup>7</sup> T. Hallman,<sup>4</sup>  
E. Hjort,<sup>10</sup> G. Igo,<sup>2</sup> P. Jacobs,<sup>7</sup> K. Kadija,<sup>13</sup> D. Keane,<sup>5</sup> L. Madansky,<sup>4</sup> C. Naudet,<sup>7</sup>  
D. Nygren,<sup>7</sup> G. Odyniec,<sup>7</sup> D. Olson,<sup>7</sup> G. Paic,<sup>13</sup> A. Poskanzer,<sup>7</sup> G. Rai,<sup>7</sup>  
H.G. Ritter,<sup>7</sup> R. Scharenberg,<sup>10</sup> L.S. Schroeder,<sup>7</sup> P. Seidl,<sup>7</sup> P. Seyboth,<sup>8</sup> D. Shy,<sup>7</sup>  
R. Stock,<sup>3</sup> T.J.M. Symons,<sup>7</sup> L. Teitelbaum,<sup>7</sup> M.L. Tincknell,<sup>9</sup> H. Van Hecke,<sup>6</sup>  
X.N. Wang,<sup>7</sup> R. Welsh,<sup>4</sup> W. Wenzel,<sup>7</sup> H. Wieman,<sup>7</sup> and K.L. Wolf<sup>11</sup>

<sup>1</sup> University of California, Davis, California 95616, U.S.A.

<sup>2</sup> University of California, Los Angeles, California 90024, U.S.A.

<sup>3</sup> University of Frankfurt, D-6000 Frankfurt am Main 90, West Germany.

<sup>4</sup> The Johns Hopkins University, Baltimore, Maryland 21218, U.S.A.

<sup>5</sup> Kent State University, Kent, Ohio 44242, U.S.A.

<sup>6</sup> Los Alamos National Laboratory, Los Alamos, New Mexico, U.S.A.

<sup>7</sup> Lawrence Berkeley Laboratory, Berkeley, California 94720, U.S.A.

<sup>8</sup> Max Planck Institute for Physics, Munich, West Germany

<sup>9</sup> Oak Ridge National Laboratory, Oak Ridge, Tennessee, U.S.A.

<sup>10</sup> Purdue University, West Lafayette, Indiana 47907, U.S.A.

<sup>11</sup> Texas A&M University, College Station, Texas 77843, U.S.A.

<sup>12</sup> University of Washington, Seattle, Washington 98195, U.S.A.

<sup>13</sup> Rudjer Boskovic Institute, 41001 Zagreb, Yugoslavia

### **Abstract**

The concept for an experiment to study global event signatures of Quark Gluon Plasma formation and to investigate the propagation of jets through strongly interacting matter at high density is presented. Both event-by-event and inclusive measurements of physical observables can be made at midrapidity over a large solid angle ( $|\eta| < 1$ ) with full azimuthal coverage ( $\Delta\phi = 2\pi$ ) and azimuthal symmetry. The detection system consists of a vertex detector and time projection chamber (TPC) inside a solenoidal magnet for tracking, momentum analysis and particle identification; a time-of-flight system surrounding the TPC for particle identification at higher momenta; and electromagnetic and hadronic calorimetry to measure and trigger on jets and the transverse energy of events.

### **I. Physics**

#### **A. Overview**

The aim of this experiment is to search for event signatures of Quark-Gluon Plasma (QGP) formation and investigate the behavior of strongly interacting matter at high energy density. The experiment utilizes two aspects of hadron production that

---

\* The author list includes all those who have contributed to the concept of this experiment. This is not necessarily the same as those who will be on the Letter of Intent.

are fundamentally new at RHIC. These are correlations between *global observables on an event-by-event basis* and the use of *hard scattering of partons* as a probe of the properties of high density nuclear matter. The event-by-event measurement of global observables - such as temperature, flavor composition, collision geometry, reaction dynamics, and energy or entropy fluctuations - is possible because of the very high charged-particle multiplicity densities ( $dn_{ch}/d\eta \approx 2000$ ) expected in nucleus-nucleus collisions at RHIC. Furthermore, measurable jet yields at RHIC will allow investigations using hard QCD processes.

Correlations between observables on an event-by-event basis can be used to isolate potentially interesting event types. A systematic study of particle and jet production would be useful over a range of colliding nuclei from pp through AA, over a range of impact parameters from peripheral to very central, and over the range of energies available at RHIC. The experiment would momentum analyze and identify charged particles ( $\pi^+$ ,  $\pi^-$ ,  $K^+$ ,  $K^-$ , p,  $\bar{p}$ , d,  $\bar{d}$ ), as well as various neutral strange particles ( $K^0$ ,  $\phi$ ,  $\Lambda$ ,  $\bar{\Lambda}$ ) via their charged-particle decay modes. High  $p_{\perp}$  jets could be identified and measured event-by-event using segmented electromagnetic and hadronic calorimetry.

## B. Products of Hard QCD Processes

The goal of studying products of hard QCD processes is to gain an understanding of the propagation of quarks and gluons in dense nuclear matter, hot hadronic matter and quark matter. Various calculations have predicted that the propagation of quarks and gluons through matter depends strongly upon properties of the matter.<sup>1,2,3,4,5</sup> A comparison of the measured yields and energies of products of hard QCD scattering processes in nucleus-nucleus collisions with predictions for their propagation through nuclear, hadronic and quark matter should furnish valuable information on the composition of the matter in these collisions.

### High $p_{\perp}$ Jets

Hard parton-parton collisions will occur within the first fm/c of the start of the nucleus-nucleus collision process.<sup>6,7</sup> To be observed at midrapidity, products of a single hard parton-parton scattering (dijets) must traverse distances of several fermi through high density matter in a nucleus-nucleus collision. The energy loss of these propagating quarks and gluons is predicted<sup>5,8</sup> to be very sensitive to the medium. Passage through hadronic or nuclear matter is predicted to result in a dampening and broadening of jets, whereas in the case of a QGP a transparency and enhanced

---

<sup>1</sup> J.D. Bjorken, Fermilab Report 82/59/59-THY (1982).

<sup>2</sup> J. Appel, Phys. Rev. D33 (1986) 717.

<sup>3</sup> J.P. Blaizot and L.D. McLerran, Phys. Rev. D34 (1986) 2739.

<sup>4</sup> M. Rammersdorfer and U. Heinz, Phys. Rev. D41 (1990) 306.

<sup>5</sup> M. Gyulassy and M. Plummer, Lawrence Berkeley Laboratory Report LBL-28531 (1990), submitted to Phys. Lett. B.

<sup>6</sup> E.V. Shuryak in Proceedings of this Workshop.

<sup>7</sup> T. Matsui in Proceedings of this Workshop.

<sup>8</sup> X.N. Wang in Proceedings of this Workshop.

yield is expected relative to the damped case. The yield of jets should be measured as a function of the transverse energy of the jet. The jet events can be correlated with other event observables to deduce information on the dynamics of the collision process. The jet studies require systematic measurements of pp interactions in addition to heavier mass systems. Systematics as a function of impact parameter for heavier systems are also particularly important.

The jet production rates at RHIC have been calculated.<sup>9</sup> For Au ions at 200 GeV/n and a luminosity of  $2 \times 10^{26} \text{ cm}^{-2}\text{sec}^{-1}$ , the expected singles rates for jets are approximately  $3 \times 10^4$ , 60 and 1 per day for  $p_{\perp} > 20$ , 40 and 60 GeV/c, respectively. These rates are somewhat independent of the mass of the beam when the luminosities as a function of the beam mass are taken into consideration.

### Mini-Jets and High $p_{\perp}$ Tails of Distributions

Mini-jets are expected to be copiously produced in collisions at RHIC.<sup>10,11</sup> As is the case for high  $p_{\perp}$  jets, the yield and topology of mini-jets is expected to be strongly influenced by the state of the high density medium through which they propagate.<sup>12</sup> However, direct measurement of mini-jets is virtually impossible due to their large opening angle and to the strongly varying background, at large particle densities, relative to the mini-jet energies. Thus, it is important to study the degree of fluctuation of the transverse energy and multiplicity as a function of rapidity and azimuthal angle ( $d^2E_{\perp}/dyd\phi$ ) of individual events, which should be strongly affected by the mini-jets.<sup>8,13</sup> Likewise, the yield and spectrum of individual hadrons at  $p_{\perp} > 3 \text{ GeV}/c$  would also be affected by modification of the jets and mini-jets by the medium. However, it should be emphasized that the single particle cross sections fall off more rapidly as a function of  $p_{\perp}$ , i.e. with  $\sigma_{\text{inv}} \sim p_{\perp}^{-8}$ , than the jet cross sections,<sup>14</sup> which fall off as  $\sigma_{\text{inv}} \sim p_{\perp}^{-5}$ .

## C. Particle Production

### Particle Spectra and Yields

The transverse momentum ( $p_{\perp}$ ) distributions of charged particles can be measured and studied inclusively with high statistics for effects such as collective radial flow<sup>15</sup> at low  $p_{\perp}$ , critical temperature<sup>16</sup> at intermediate  $p_{\perp}$ , and mini-jet attenuation<sup>8</sup> at high  $p_{\perp}$ . Comparison of these spectra for pp and AA as a function of impact parameter is important. Large unexplained differences in spectral shapes

---

<sup>9</sup> T. Ludlam, L. Madansky and F. Paige, Proc. of LBL Workshop on detectors for Relativistic Nuclear Collisions, ed. L.S. Schroeder, Lawrence Berkeley Laboratory Report LBL-18225 (1984) 115.

<sup>10</sup> K. Kajantie, P.V. Landshoff and J. Lindfors, Phys. Rev. Lett. 59 (1987) 2527.

<sup>11</sup> K.J. Eskola, K. Kajantie and J. Lindfors, Nucl. Phys. B323 (1989) 37.

<sup>12</sup> P.V. Landshoff, Nucl. Phys. A498 (1989) 217; X.N. Wang, Lawrence Berkeley Laboratory Report LBL-28790 (1990), submitted to Phys. Rev. D.

<sup>13</sup> X.N. Wang, Lawrence Berkeley Laboratory Report LBL-28789 (1990), submitted to Phys. Lett. B.

<sup>14</sup> see W. Geist et al., CERN/EP Report 89-159 (1989) to be published in Phys. Rep. (1990).

<sup>15</sup> P.V. Ruuskanen, Z. Phys. C38 (1988) 219.

<sup>16</sup> L. Van Hove, Phys. Lett. 118B (1982) 138; K. Redlich and H. Satz, Phys. Rev. D33 (1986) 3747.

have been measured in pp,  $\alpha\alpha$  and higher mass nucleus-nucleus collisions at the CERN ISR and SPS.<sup>17,18</sup> At RHIC, because of the high multiplicities in central nucleus-nucleus events, the slope of the  $p_{\perp}$  distribution for pions and the  $\langle p_{\perp} \rangle$ 's for pions and kaons can be determined event-by-event. Thus, individual events can be characterized by temperature to search for events with extremely high temperature, predicted<sup>19</sup> to result from deflagration of a QGP. Displayed in Fig. 1 are two spectra generated from Boltzmann distributions with  $T = 150$  and  $250$  MeV each containing 1000 pions. This is the average number of pions of a given charge sign expected in the acceptance  $|\eta| < 1$  of this experiment for central Au + Au collisions. The slopes of spectra with  $T = 150$  and  $250$  MeV can easily be discriminated at the single event level. Fig. 2a shows the standard deviation in measuring  $\langle p_{\perp} \rangle$  as a function of the charged particle multiplicity measured in a single event. From Fig. 2a it can be seen that the determination of  $\langle p_{\perp} \rangle$  for pions and that for kaons (for 200 charged kaons per event in the acceptance) can be made very accurately on the single event basis in this experiment.

The difference between the  $p_{\perp}$  spectra obtained for  $\Lambda$  and  $\bar{\Lambda}$  or  $p$  and  $\bar{p}$  should be indicative of the distribution in phase space of valence quarks originating from the initial nucleons of the target and projectile. The amount of net charge and net baryon number, which are proportional, reveals the stopping power of quarks and determines the baryo-chemical potential  $\mu_B(y)$  in the medium.<sup>20</sup>

### Fluctuations in Energy, Entropy and Transverse Momentum

The large energy, entropy and multiplicity densities at midrapidity in central collisions allow event-by-event measurement of fluctuations in the transverse energy ( $E_{\perp}$ ), entropy and flavor flow of different types of particles as a function of  $p_{\perp}$ , rapidity and azimuthal angle. They also allow measurements of local fluctuations in  $p_{\perp}$  as a function of rapidity and azimuthal angle. The study of these fluctuations may reveal aspects of the existence and hadronization of a QGP.<sup>21</sup> In addition, inclusive measurements of the  $E_{\perp}$  and multiplicity distributions at midrapidity provide information on the energy and matter densities, respectively.

### Flavor Composition

One of the first predictions of signatures for the existence of a QGP was an enhancement in the production of strange particles<sup>22</sup> resulting from chemical

<sup>17</sup> W. Bell et al., Phys. Lett. 112B (1982) 271; A. Karabarbounis et al., Phys. Lett. 104B (1981) 75; A.L.S Angelis et al., Phys Lett. 116B (1982) 379.

<sup>18</sup> J.W. Harris et al., Nucl. Phys. A498 (1989) 133c.

<sup>19</sup> E.V. Shuryak and O.V. Zhironov, Phys. Lett. B89 (1980) 253; E.V. Shuryak and O.V. Zhironov, Phys. Lett. B171 (1986) 99.

<sup>20</sup> R. Anishetty, P. Koehler and L. McLerran, Phys. Rev. D22 (1980) 2793; W. Busza and A.S. Goldhaber, Phys. Lett. 139B (1984) 235; S. Date, M. Gyulassy and H. Sumiyoshi, Phys. Rev. D32 (1985) 619.

<sup>21</sup> M. Gyulassy, Nucl. Phys. A400 (1983) 31c; L. Van Hove, Z. Phys. C27 (1985) 135.

<sup>22</sup> R. Hagedorn and J. Rafelski, Phys. Lett. 97B (1980) 180; J. Rafelski and B. Mueller, Phys. Rev. Lett. 48 (1982) 1066; P. Koch, B. Mueller and J. Rafelski, Phys. Rep. 142 (1986) 167.

equilibrium of a system of quarks and gluons. A measurement of the  $K/\pi$  ratio provides information on the relative concentration of strange/nonstrange quarks, i.e.  $\langle (s + \bar{s}) / (u + \bar{u} + d + \bar{d}) \rangle$ . This has been suggested<sup>23</sup> as a diagnostic tool to differentiate between hadronic gas, QGP formation and the role of the expansion velocity. This ratio can be measured very accurately on an inclusive basis and with sufficient accuracy event-by-event to classify the events for cross-correlations with other event observables. This can be seen in Fig. 2b where the standard deviation of the measured  $K/\pi$  ratio event-by-event is plotted as a function of the charged particle multiplicity measured in the event.

The production cross section of  $\phi$ -mesons can be measured inclusively from the decay  $\phi \Rightarrow K^+ + K^-$ . Measurement of the yield of the  $\phi$ , which is an  $s\bar{s}$  pair, places a more stringent constraint on the origin of the observed flavor composition<sup>24</sup> than the  $K/\pi$  ratio and is expected to be more sensitive to the presence of a QGP.

Measurement of the multiplicities of  $\Lambda$ ,  $\bar{\Lambda}$  and multiply-strange baryons requires detection of secondary decay vertices. Due to the short decay lengths, a vertex detector close to the beam axis is necessary for these measurements. The measurements provide a better determination of the strange/nonstrange quark ratio than the  $K/\pi$  ratios. Like the  $\phi$ , multiply-strange baryons are more sensitive to the existence of a QGP<sup>25</sup> than singly-strange particles.

#### Particle Correlations (Bose-Einstein and Speckle Interferometry)

Correlations between identical bosons provide information on the freezeout geometry,<sup>26</sup> the expansion dynamics<sup>27</sup> and possibly the existence of a QGP.<sup>28</sup> These correlations can be measured on an event-by-event basis for like-sign charged pions and on an inclusive basis for like-sign charged kaons and pions. With high statistics over many events the dependence of the source parameters as a function of the transverse momentum components of the particle pairs will be measured. On an event-by-event basis the source parameters can be determined from the pion correlations and correlated with other event observables. Displayed in Fig. 2c are the number of like-sign pion pairs in a single event as a function of the measured charged-particle multiplicity in the event. The two-pion correlation statistics for a single central Au + Au event at RHIC will be similar to the accumulated statistics published in most papers on the subject. However, since pion source sizes may be as large as 30 fm., the correlation in momentum space will be limited to very small differences in momentum of the pion pair. This could make event-by-event analysis of such large source sizes extremely difficult, due to the limited pair statistics

<sup>23</sup> N.K. Glendenning and J. Rafelski, Phys. Rev. C31 (1985) 823; K.S. Lee, M.J. Rhoades-Brown and U. Heinz, Phys. Rev. C37 (1988) 1452.

<sup>24</sup> A. Shor, Phys. Rev. Lett. 54 (1985) 1122.

<sup>25</sup> J. Rafelski, Phys. Rep. 88 (1982) 331.

<sup>26</sup> F.B. Yano and S.E. Koonin, Phys. Lett. B78 (1978) 556; K. Kolehmainen and M. Gyulassy, Phys. Lett. B180 (1986) 203; A. Bamberger et al., Phys. Lett. B203 (1988) 320; B. Andersson and W. Hofmann, Phys. Lett. B169 (1986) 364.

<sup>27</sup> A. Bamberger et al., Phys. Lett. B203 (1988) 320; R. Stock, University of Frankfurt Preprint (1990).

<sup>28</sup> S. Pratt, Phys. Rev. D33 (1986) 1314; G. Bertsch, M. Gong and M. Tohyama, Phys. Rev. C37 (1988) 1896 and G. Bertsch MSU Preprint (1988).

at small momentum differences. It also places stringent constraints on the two particle-track resolution. To supplement the two-particle correlation data, higher particle number correlations can also be analyzed.

Inclusive measurement of KK correlations should complement the  $\pi\pi$  correlation data since K's are expected to freeze out earlier<sup>29</sup> during expansion than the  $\pi$ 's. Also, depending upon the baryo-chemical potential and the existence of a QGP, the  $K^+$  and  $K^-$  are expected to freeze out at different times.<sup>29</sup> Furthermore, the KK correlation is less affected by resonance decays after hadronic freeze-out than the pion correlations<sup>30</sup>, thus making interpretation of the KK correlation data easier.

With the high pion density in phase space, unique to RHIC, a novel aspect of multi-pion clustering analogous to optical speckle interferometry<sup>31</sup> should be observable for the first time.<sup>32</sup> These "speckles" are a collective multi-particle effect which leads to macroscopic structure in phase space. They may offer information on the hadronic source which is complementary to that deduced from traditional Bose-Einstein pair correlation analysis. However, prior to any interpretation of "speckle interferometry" data, significant theoretical progress on the Coulomb multiparticle corrections is necessary,

### **Expansion Dynamics**

Anti-deuterons and heavier anti-nuclei can result from the coalescence of combinations of  $\bar{p}$  and  $\bar{n}$  during expansion when the antinucleon density reaches freezeout density. The "coalescence ratio"  $\langle \bar{d} \rangle / \langle \bar{p} \rangle^2$  not only depends on the dynamics of source expansion (radial flow, temperature, etc.) at this stage but also on the source size, which reduces this ratio with increasing radius. This observable can provide information complementary to the particle correlation analysis.<sup>33</sup>

### **Correlations between Event Observables**

It should be emphasized that the capability of characterizing events in terms of the values of observables measured event-by-event is unique to this experiment. Events can be characterized by their temperature, flavor content, source size, transverse energy density, multiplicity density, entropy density and degree of fluctuations. Events with extreme values of these observables may be of special interest.

## **II. Detecting and Measuring Jets at RHIC**

Various methods of generating jet events, studying properties of jets and measuring jets in nucleus-nucleus collisions at RHIC have been investigated.

---

<sup>29</sup> K.S Lee, M.J. Rhoades-Brown and U. Heinz, Phys. Rev. C37 (1988) 1463.

<sup>30</sup> M. Gyulassy and S. S. Padula, Lawrence Berkeley Laboratory Report LBL-26077 (1988).

<sup>31</sup> A. Labeyrie in Progress in Optics, ed. E. Wolf, North-Holland Publishing Co., Amsterdam Vol. 14 (1976).

<sup>32</sup> W.A. Zajc, Phys. Rev. D35 (1987) 3396.

<sup>33</sup> S. Mrowczynski, Regensburg Report (1990) to be published in Phys. Lett.

Displayed in Fig.3a is a 40 GeV dijet event generated by Isajet<sup>34</sup> for a  $\sqrt{s} = 200$  GeV pp collision as viewed by the calorimeters in  $E_{\perp}$  vs  $\phi$  and  $\eta$  space. The two jets are easily identified and their energies and directions measured. When this same hard parton-parton scattering is mixed into a  $\sqrt{s} = 200$  GeV/n Au + Au event, generated by the Lund/Fritiof nucleus-nucleus code<sup>35</sup> at impact parameter  $b = 0$ , the resulting plot of  $E_{\perp}$  vs  $\phi$  and  $\eta$  in the calorimeters is shown in Fig. 3b. Jets in the background of a central Au + Au event are qualitatively more difficult to find and measure. The CDF jet-finding algorithm<sup>36</sup> was used to study the feasibility of identifying and measuring jets in collisions at RHIC. The results are summarized in Fig. 4. Displayed in Fig. 4a are the efficiencies for finding one and both jets of a pair in the nucleus-nucleus background as a function of the  $E_{\perp}$  of the jet. The efficiencies increase as the  $E_{\perp}$  of the jet increases. Displayed in Fig. 4b is the measured  $E_{\perp}$  of the jet as a function of the  $E_{\perp}$  of the jet known from the simulation. The measured  $E_{\perp}$  is extracted from the background by subtraction of the average background  $E_{\perp}$  from the locus of the jets determined from the jet-finder. The error bars shown in Fig. 4b are the standard deviations of the measurements, without effects of detector resolution. Displayed in Fig. 4c are the standard deviations for determination of  $\phi$ ,  $\eta$ , and  $E_{\perp}$  for jets in the simulations. The jet energies can be well determined on the average, but fluctuations of the background increase the error in the measurements over those measured in pp interactions. Determination of the jet direction is less affected by the background and the accuracy less important than the jet  $E_{\perp}$  determination. Precise determination of  $E_{\perp}$  is critical because of the steeply falling jet cross section as a function of jet  $E_{\perp}$ .

Some of the problems associated with jet finding may be solved by improvement and careful tuning of the jet-finding algorithms, particularly the energy determination, for the nucleus-nucleus environment. Likewise, careful consideration of the function and design of the calorimetry is necessary to improve the jet energy signal/background. Perhaps the most complicated and most important effect is that of misidentifying fluctuations of the soft background as jets. This requires further investigation.

Wang and Gyulassy have developed a code to simulate nucleus-nucleus collisions at RHIC using as a basis the Pythia code<sup>37</sup> for pp interactions plus inclusion of the nucleus-nucleus geometry. Partons are propagated through the matter in the collision and their energy loss is calculated depending upon the type of matter traversed (partonic, hadronic or QGP). Results from these simulations exhibit a strong attenuation of jets and mini-jets in hadronic matter. The attenuation decreases dramatically for traversal of deconfined matter (QGP). The results of the calculations are very much dependent upon the dynamics of the collisions, but the effects are largest at midrapidity. A detailed study of the effects of mini-jet and jet attenuation on the transverse energy measured in calorimetry is underway.

---

<sup>34</sup> F.E. Paige and S.D. Protopopescu, ISAJET, Brookhaven National Laboratory Report BNL-37066 (1985).

<sup>35</sup> B. Andersson et al., Nucl. Phys. B281 (1987) 289.

<sup>36</sup> F. Abe et al., Phys. Rev. Lett. 62 (1989) 613.

<sup>37</sup> T. Sjostrand and M. van Zijl, Phys. Rev. D36 (1987) 2019.

Effects on the jet energy resolution of momentum cutoffs due to magnetic fields, absorption and subdivision of the measured energy into electromagnetic and hadronic fractions have been investigated using the Pythia simulation code. These calculations indicate that independent determination of EM or hadronic energy alone is insufficient for accurate jet energy determination, due mainly to the low particle statistics (10-15) in the jet. The primary source of fluctuations of the background is minijets.

The use of both jets in a dijet event allows better identification. Furthermore, measuring the dijet momentum balance provides additional information which may be useful in determining the presence of a QGP. A measurement of the two-jet differential cross section for nucleus-nucleus collisions may in itself be of interest to understanding the parton fragmentation functions in hadronic matter.

### **III. Layout of Experiment**

#### **A. Overview**

The physics goals were used to specify the design of the experiment. The experiment consists of tracking, particle identification and calorimetry at midrapidity over a large solid angle ( $|\eta| < 1$ ) with full azimuthal coverage ( $\Delta\phi = 2\pi$ ) and azimuthal symmetry. The detection system consists of a vertex detector to locate the primary and secondary vertices and a time projection chamber inside a solenoidal magnet for tracking, momentum analysis and particle identification; a time-of-flight system surrounding the TPC to extend particle identification to higher momenta than achievable using  $dE/dx$  alone; and electromagnetic and hadronic calorimetry to measure and trigger on jets and the transverse energy of events. A diagram of the experiment is shown in Fig. 5.

#### **B. Magnetic Field**

The magnet is a solenoid with uniform magnetic field along the beam direction. This magnet design is chosen for complete azimuthal symmetry and high tracking accuracy. A field strength of 0.5 Tesla provides adequate resolution for momenta as high as 10 GeV/c with only modest spiralling of low  $p_{\perp}$  particles. With a TPC inner radius of 0.5 m. the acceptance extends to transverse momenta as low as 40 MeV/c. The magnetic coil radius is 2 m. and the radius of the yoke 4 m., both 8m. in length. The magnet is a room temperature design which minimizes the coil thickness.

#### **C. Charged Particle Tracking System**

Momentum analysis and particle identification of all charged particles at midrapidity are necessary to achieve the physics goals of the experiment. The tracking should operate in conditions at higher than the maximum track density,  $dn_{ch}/dy = 1500$ , and multiplicity,  $n_{ch} = 3000$ , in the  $|\eta| < 1$  acceptance of the experiment expected for central Au + Au collisions. Momentum resolution of  $\Delta p/p < 0.01$  at  $p = 0.1$  GeV/c is required by two-particle correlations, and  $\Delta p/p < 0.02$  at  $p = 10$  GeV/c is necessary to accurately measure spectra at high  $p_{\perp}$  and particles from mini-jets and jets. Particle identification of pions/kaons/protons over momenta  $p < 3$  GeV/c and measurement of decay particles from secondary vertices should be

possible. An additional constraint on the tracking resolution specified by the particle identification resolution is  $\Delta p/p = (0.01 \times p)$  for  $p < 3 \text{ GeV}/c$ . It is anticipated that the momentum resolution for high  $p_{\perp}$  can be improved by further design, optimization and integration of the tracking detectors.

### **Time Projection Chamber (TPC)**

The TPC consists of two sections each 2.5 m long as shown in Fig. 5. Ionization will drift to two end-caps, located on the outer ends. Each end-cap is instrumented with 75,000 pads, each of dimension 8mm x 20mm. Each pad receives 512 time samples. Singly-charged particles with  $p_{\perp} < 40 \text{ MeV}/c$  spiral inside the inner TPC radius of 50 cm. and do not reach the TPC. Particles with  $40 \text{ MeV}/c < p_{\perp} < 150 \text{ MeV}/c$  spiral inside the TPC and most exit the end-caps. Particles with  $p_{\perp} > 150 \text{ MeV}/c$  traverse the TPC and exit the outer edge at radius 200 cm. Details of the TPC design can be found in Table 1.

The gas inside the TPC is expected to be neon in order to reduce multiple scattering which dominates the momentum resolution at low momentum. The momentum resolution is displayed in Fig. 6a for the low momenta and Fig. 6b for the high momentum range of the experiment. These were calculated for the TPC using neon gas, without vertex determination. The momentum resolution at high momentum is dictated by the two track resolution at the outer radius of the TPC for two tracks close in both momentum and coordinate space.

### **Vertex Detector (VTX)**

The function of the Vertex Detector, coupled with the TPC, is to locate the position of the primary interaction vertex, to improve the momentum resolution for high momentum tracks and to locate secondary vertices with approximately 1mm accuracy. The VTX must be able to provide three dimensional space points and vectors for traversing tracks with high spacial resolution. These tracks can be linked to tracks measured in the TPC. To cover  $|\eta| < 1$  the VTX is located at a radius of approximately 0.1 m. from the beam and has a length of 0.5 m., as shown in Fig. 5.

The design of the VTX depends upon developments in silicon detector technology.<sup>38,39</sup> It should be cylindrical in shape and either a multilayer pixel detector or a superlayer strip detector with stereo layers. Silicon technology should be able to provide a detector with approximately 300,000 pixels of size  $1\text{mm}^2$  per layer. The VTX must be of low mass so as to minimize secondary particle production, secondary interactions and multiple scattering.

### **D. Time-of-Flight (TOF) Detector System**

To supplement the particle identification capability of the TPC, which is mainly at momenta  $p < 0.8 \text{ GeV}/c$ , a TOF system is used. This extends the particle identification up to approximately 2-3 GeV/c in momentum depending upon the particle. A summary of the specifications of the TOF system is provided in Table 2. The particle

<sup>38</sup> S. Parker, Nucl. Instr. Meth. A275 (1989) 494.

<sup>39</sup> "SSC Detector R&D Proposal: Development of Technology for Pixel Vertex Detector," D. Nygren - spokesperson (1989).

Identification that can be achieved with the TPC - TOF system combination is displayed in Fig. 7. The region outside the largest semi-circle ( $3\sigma$  separation) constitutes the allowed region. The calculations assume a 2 m. flight path and  $\sigma = 170$  ps for the entire TOF system. With a slightly improved time resolution ( $\sigma = 100$  ps) the TPC-TOF combination would meet the overall requirements for particle identification. At a distance of 2 m. from the beam, the TOF system with a  $6 \text{ cm}^2$  pixel size and 100,000 pixels has a maximum occupancy factor of 2 percent.

The TOF system has not been designed. A TOF system that operates in the magnetic field is preferred. Due to the high segmentation (100,000), lower cost detector systems than presently available must be developed.

### **E. Midrapidity Calorimeters**

The primary purpose of the midrapidity calorimeters is to measure and trigger on high  $p_{\perp}$  jets and the transverse energy of events. The calorimeters consist of separate electromagnetic and hadronic sections with a lateral segmentation of  $\Delta\phi = 10^\circ$  and  $\Delta\eta = 0.1$ , for a total of 720 towers. The inner diameter will be 2.5 m. and outer diameter 3.8 m. Fig. 5 displays the calorimetry relative to the other detectors in the experiment. The necessity to measure precisely the transverse energies suggests the use of a compensated calorimeter with a linear response down to low energies. Corrections to the calorimeter measurements for distortions of the trajectories of charged particles in the magnetic field can be made using the tracking data.

#### **Hadronic**

The hadronic calorimetry consists of Pb/scintillator sandwich (1 cm. Pb, 2 mm. plastic scintillator) with energy resolution of approximately  $0.35-0.40/\sqrt{E}$ . The modules are designed to point towards the interaction vertex region and are 6 interaction lengths deep. The lateral segmentation may change after more extensive simulations are completed.

#### **Electromagnetic**

The design of the electromagnetic (EM) calorimeters has yet to be determined. It should be noted that an appreciable fraction of the deposited energy is in low energy charged pions. There is little or no difference in shower profiles for charged pions vs EM showers for these low incident energies. The effect of the magnetic field must be considered in the design. The most straightforward choice for the EM calorimeters is to utilize a section of the same Pb/scintillator sandwich structures which form the hadronic section. The EM section would be approximately 0.3 to 1.2 interaction lengths thick, depending upon the jet resolution and calorimeter simulations. In practice, a compensated section with the same response as the hadronic section produces a system which is much easier to construct and calibrate than a high resolution EM section. The EM energy resolution is expected to be approximately  $0.22/\sqrt{E}$ .

For better jet energy resolution the burden rests on the design of the EM section which must operate in high background. The effect of the lateral segmentation and

energy resolution of the EM section of the calorimetry requires more investigation. A lateral segmentation identical to that of the hadronic segmentation will be simulated.

### **F. Intermediate Rapidity ( $1 < |\eta| < 5$ ) Detectors**

The region  $|\eta| > 1$  is presently unspecified. An extension of the calorimetry to  $|\eta| < 1.5 - 2$  is being considered to improve the definition of jets. Since jets are observed to spread energy over a region of pseudorapidity ( $\eta$ ) and azimuthal angle ( $\phi$ ) of size approximately  $\sqrt{(\Delta\eta)^2 + (\Delta\phi)^2} = 1$  about the direction of the jet, edge effects are minimized by calorimeter coverage extending beyond  $|\eta| = 1$ . For event characterization, full calorimeter coverage is preferred. Likewise, there are similar event characterization arguments for expanding the charged particle multiplicity coverage to include the region  $1 < |\eta| < 5$ . Insights into these possibilities are being sought from simulations.

### **G. Triggering**

The triggering scheme is still being developed. A three level trigger is anticipated. The first level trigger will consist of decisions at the "hardware" level. Several parallel triggers are expected at this level - multiplicity,  $E_{\perp}$ , forward energy, total energy and various ratios of these quantities. First level decisions are made in less than a  $\mu$ second. The TPC readout and digitization of counters commence on this trigger. The second level trigger is decided in tens of  $\mu$ seconds. It could consist of topological configurations of interest from the detectors, such as single jets, back-to-back jets, or fluctuations of various observables. The third level trigger operates on a timescale of milliseconds up to seconds. It should consist of trackfinding, momentum reconstruction, particle identification and data compression. It should be noted that the various parallel triggers will be prioritized such that triggers with the smallest cross sections can receive priority interrupts.

### **H. Spectator Calorimeter**

A spectator calorimeter to measure the forward energy at rapidities near that of the beam must be developed. This is a detector that might be common to all experiments. The forward energy information from a spectator calorimeter can be correlated with the midrapidity calorimeters to characterize events by the centrality of the nucleus-nucleus collisions.

### **I. Data Acquisition Rates**

At present the maximum expected data acquisition rates for this experiment range from 1 central Au + Au interaction per second to 10 minimum bias Au + Au interactions per second, limited by data acquisition and storage rates. The event size for central Au + Au collisions is expected to be 80 MB. After reduction by the maximum filling factor expected for the TPC (10%) this becomes 8 MB per event. It is possible that with some developments in data reduction and compression the data rate could be increased, as much as tenfold.

## **J. Data Acquisition Philosophy**

The goals of this experiment require data acquisition utilizing a range of projectiles (from protons to Au), available beam energies and impact parameters. It is expected that longer data acquisition periods will be necessary for studies of jet production in  $p + p$ ,  $Au + Au$  and an intermediate mass system. Furthermore, the data acquisition requirements of this experiment are inherently different from those of experiments which measure observables with small cross sections. Those experiments will require data accumulation with a fixed projectile and energy for as long as possible.

## **Acknowledgements**

The authors wish to thank N.K. Glendenning, A. Shor, G. Young, T. Ludlam, W. Geist, R. Kadel, S. Nagamiya, W. Carithers, J. Siegrist, M. Shapiro, B. Jacak and L. Van Hove for interesting and helpful discussions. This work was supported in part by the Director, Office of Energy Research, Division of Nuclear Physics of the Office of High Energy and Nuclear Physics of the U.S. Department of Energy under contract DE-AC03-76SF00098.

## **Appendix - RHIC Detector R&D Projects**

Several detector R&D projects are necessary for the success of this concept. One project, already funded, is to develop *Integrated TPC Electronics* which includes preamp, shaper, analog storage and ADC on a single integrated circuit. Development of high resolution ( $\sigma \sim 100$  ps) time-of-flight detectors, which are inexpensive compared to the cost of photomultiplier tubes, is important when considering 100,000 channels of detectors. In addition, possible operation in a magnetic field has led to consideration of *Pestov Spark Counters* and *Silicon Avalanche Diodes* for development. A project is underway to study the feasibility of a *High Track Pair Resolution TPC* which uses a parallel plate avalanche readout with resistive mesh to increase the two-track resolution, possibly tenfold. To be able to increase the data acquisition rate *Online Data Compression* via specialized hardware for track processing and analysis will be pursued. The development of a *Vectoring Vertex Detector* is necessary for this and possibly other RHIC experiments. Either a pixel vertex detector system or one with silicon superlayer strips will be developed. The calorimetry must be designed and the *Calorimeter Readout* optimized for use in this experiment. Various readout techniques, for example the use of wavelength shifter (WS) bars or WS fiber optics, will be investigated. For calibration of the TPC a unique *3-D TPC Laser Calibration System*, utilizing time modulation of ultraviolet laser light to produce three-dimensional space points of ionization in the TPC, will be developed.

## Tables

Table 1. TPC Detector Specifications

### **Tracking - Time Projection Chamber**

Two Sections	
Uniform field (solenoid)	$B = 0.5 \text{ T}$
Inner radius	0.5 m
Outer radius	2.0 m
Length of each section	2.5 m
# pads at each of 2 endcaps	75,000
Pad size	8mm x 20 mm
Tracking accuracy	100 $\mu\text{m}$
Time samples	512
Drift time	50 $\mu\text{sec}$
Maximum interaction rates	$10^4$ /sec Au-Au, $10^6$ /sec p-p

Table 2. Time-of-Flight Detector Specifications

### **Time-of-Flight**

Radius	2 m
Area	60 $\text{m}^2$
Cell occupancy	$< 0.02$
Pixel size	6 $\text{cm}^2$
Channels required	100,000
Time resolution	$< 100 \text{ psec}$
Channel dead-time	$< 1 \text{ msec}$

## Figures

### **Figure Captions**

1. Simulation of  $dn/dp_{\perp}$  vs.  $p_{\perp}$  for an event generated using a Boltzmann distribution with 1000 pions. The curves correspond to single events generated with  $T = 150 \text{ MeV}$  and  $250 \text{ MeV}$ , as labelled.

2. As a function of the charged-particle multiplicity measured in an event are plotted a) the standard deviation of  $p_{\perp}$ , b) the standard deviation of the ratio  $K/\pi$  (assuming  $\langle K/\pi \rangle = 0.1$ ) and c) the number of like-sign pion pairs. A central Au + Au

event at RHIC is expected to produce 2000 charged particles (1000 pions of each charge) into the acceptance of this experiment.

3. a) A plot of  $dE_{\perp}$  vs  $\phi$  and  $\eta$  of a 40 GeV dijet event generated by Isajet for a  $\sqrt{s} = 200$  GeV pp collision. b) A plot of  $dE_{\perp}$  vs  $\phi$  and  $\eta$  for the same hard parton-parton scattering mixed into a  $\sqrt{s} = 200$  GeV/n Au + Au event, generated at impact parameter  $b = 0$  by the Lund/Fritiof nucleus-nucleus code. A lateral segmentation of  $\Delta\phi = 10^{\circ}$  and  $\Delta\eta = 0.1$  for the calorimetry is assumed. No effects of detector resolution have been input into this calculation.

4. a) The efficiency for finding dijets in a simulation using the CDF jet-finding algorithm plotted as a function of the transverse energy  $E_{\perp}$  of the jet. A lateral segmentation of  $\Delta\phi = 10^{\circ}$  and  $\Delta\eta = 0.1$  of the calorimeters is assumed. The 400 events were generated using the Lund/Fritiof model for  $\sqrt{s} = 200$  GeV/n Au + Au at impact parameter  $b = 0$  and superimposing dijets generated with Isajet at the same incident energy. Plotted are the efficiencies for finding one jet of the pair  $\epsilon_{1,2}$  and both jets of the pair  $\epsilon_2$ . Also plotted is a point for the efficiency for finding jets in a pp event with the same code. No detector resolution has been input into the calculation. b) The measured transverse energy  $E_{\perp}$  of the jet as a function of the actual transverse energy  $E_{\perp}$  of the jet for the same sample of events. c) The standard deviations in determining the azimuthal angle  $\phi$ , pseudorapidity  $\eta$  and transverse energy  $E_{\perp}$  of the jet as a function of the jet transverse energy  $E_{\perp}$ .

5. Conceptual layout of the experiment. See text for description.

6. Momentum resolution for two ranges of momenta.

7. Particle identification using a combination of energy loss and time-of-flight.<sup>40</sup> Displayed is the time difference and energy loss difference between pairs of particles (K-p, K- $\pi$ ,  $\pi$ -p). The 3 lines correspond to the 3 types of particle pairs considered. The momentum of the particles is given along each line. The semi-circles correspond with increasing radii to 1, 2 and 3 $\sigma$  separation, respectively. The region outside the semi-circles represents the allowed-region. The calculations assume 2 m. flight path and 170 ps time resolution for the time-of-flight system.

---

<sup>40</sup> H.G. Pugh, G. Odyniec, G. Rai and P. Seidl, Lawrence Berkeley Laboratory Report LBL-22314 (1986).

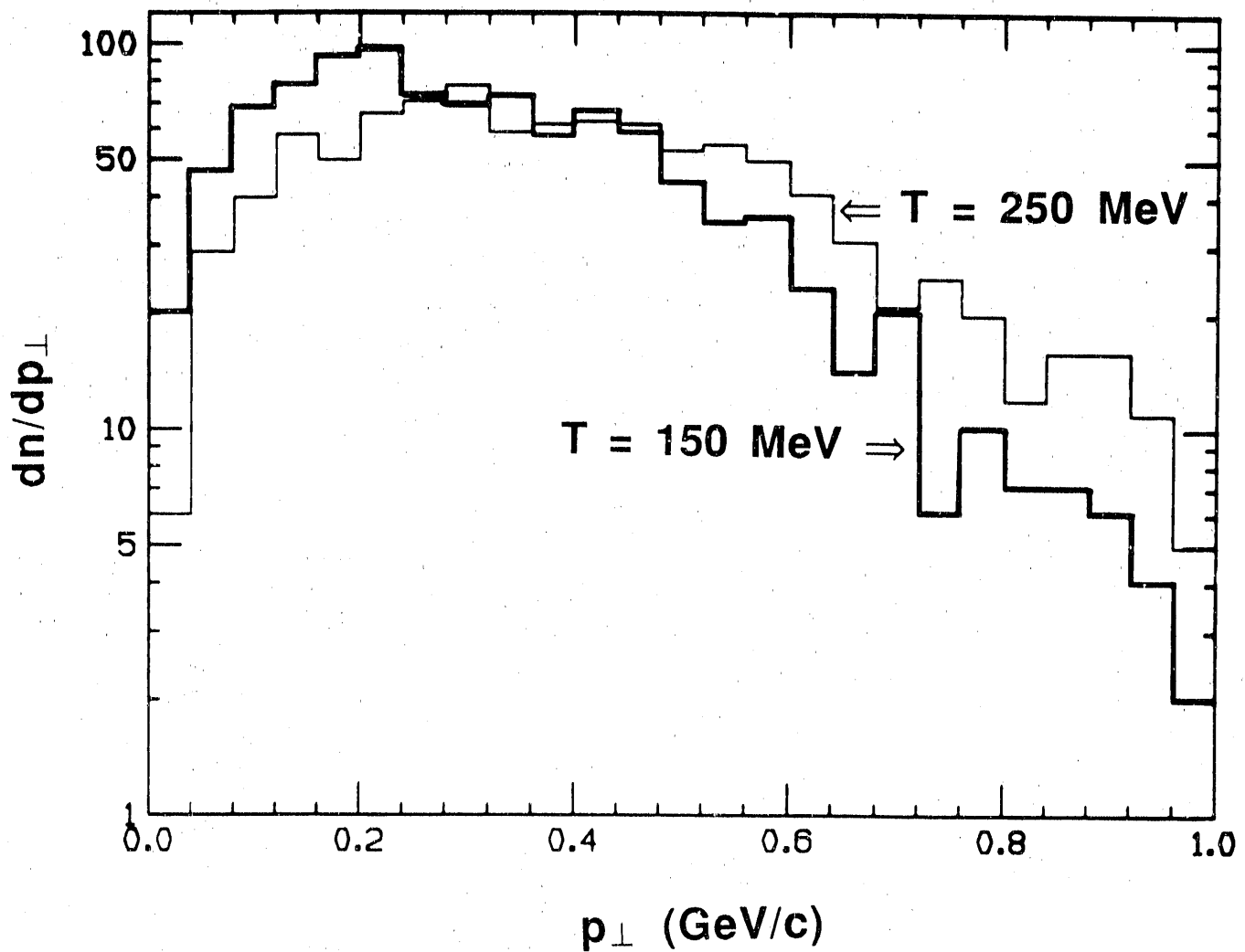


Fig. 1

# Event by Event Physics

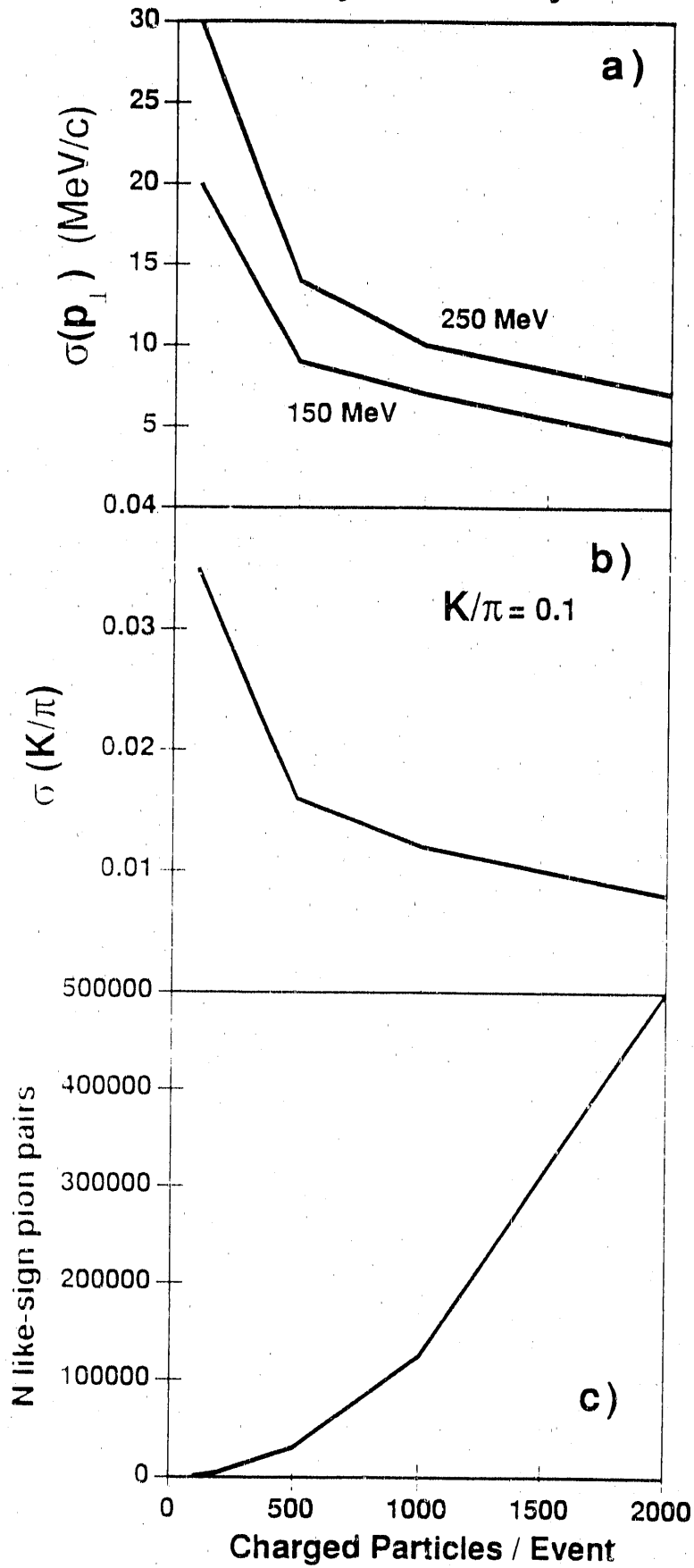
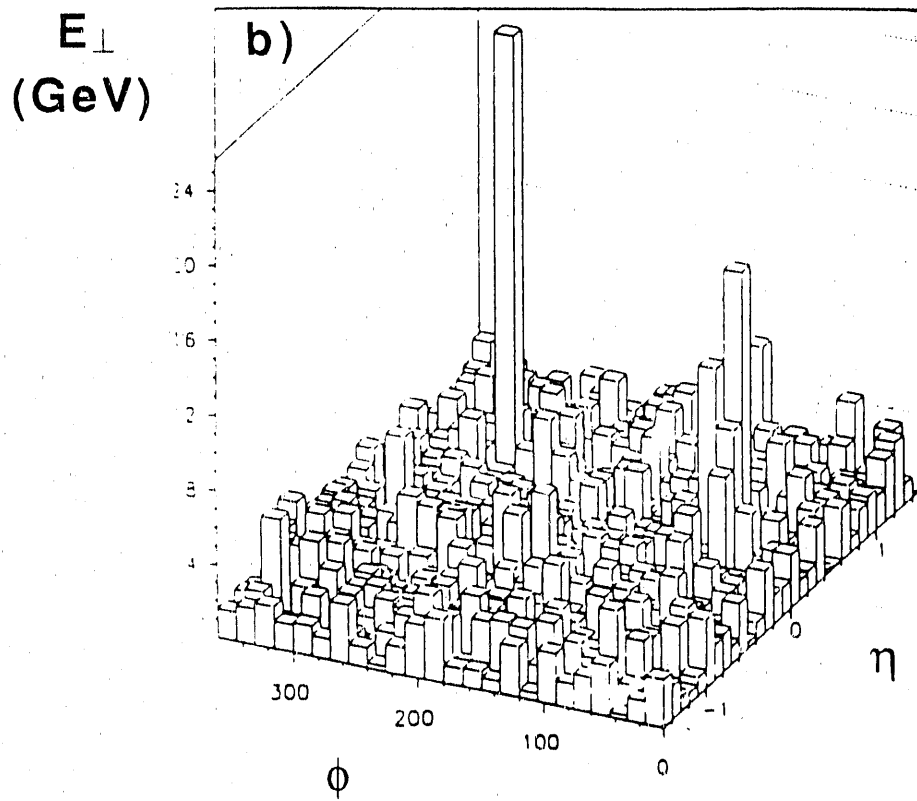
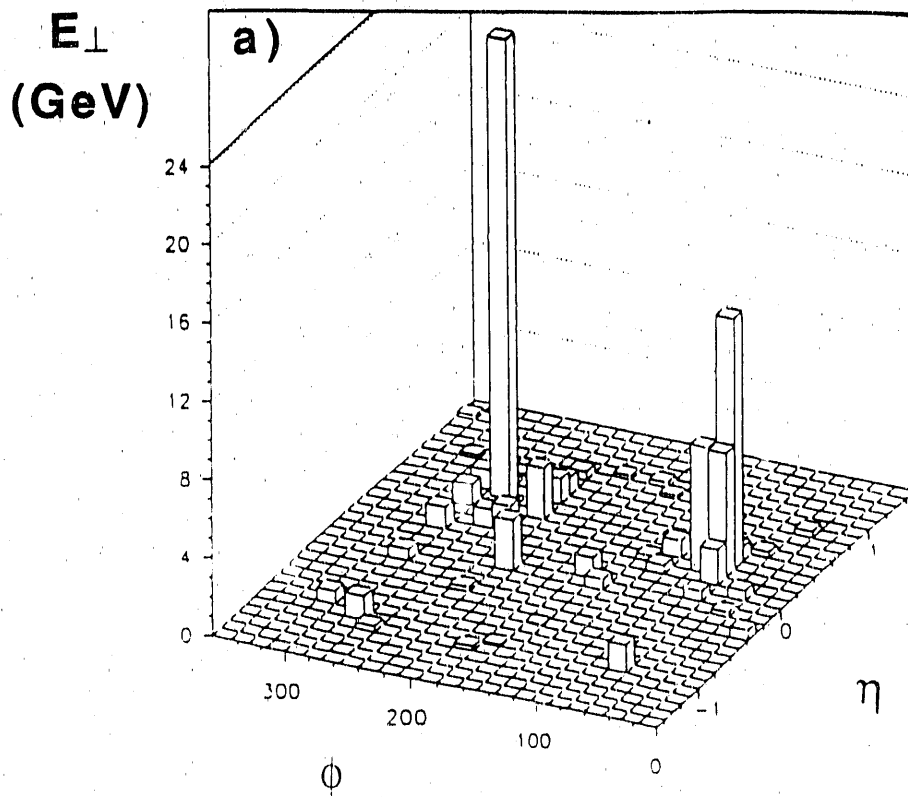


Fig. 2



**Fig. 3**

# Jet Finding

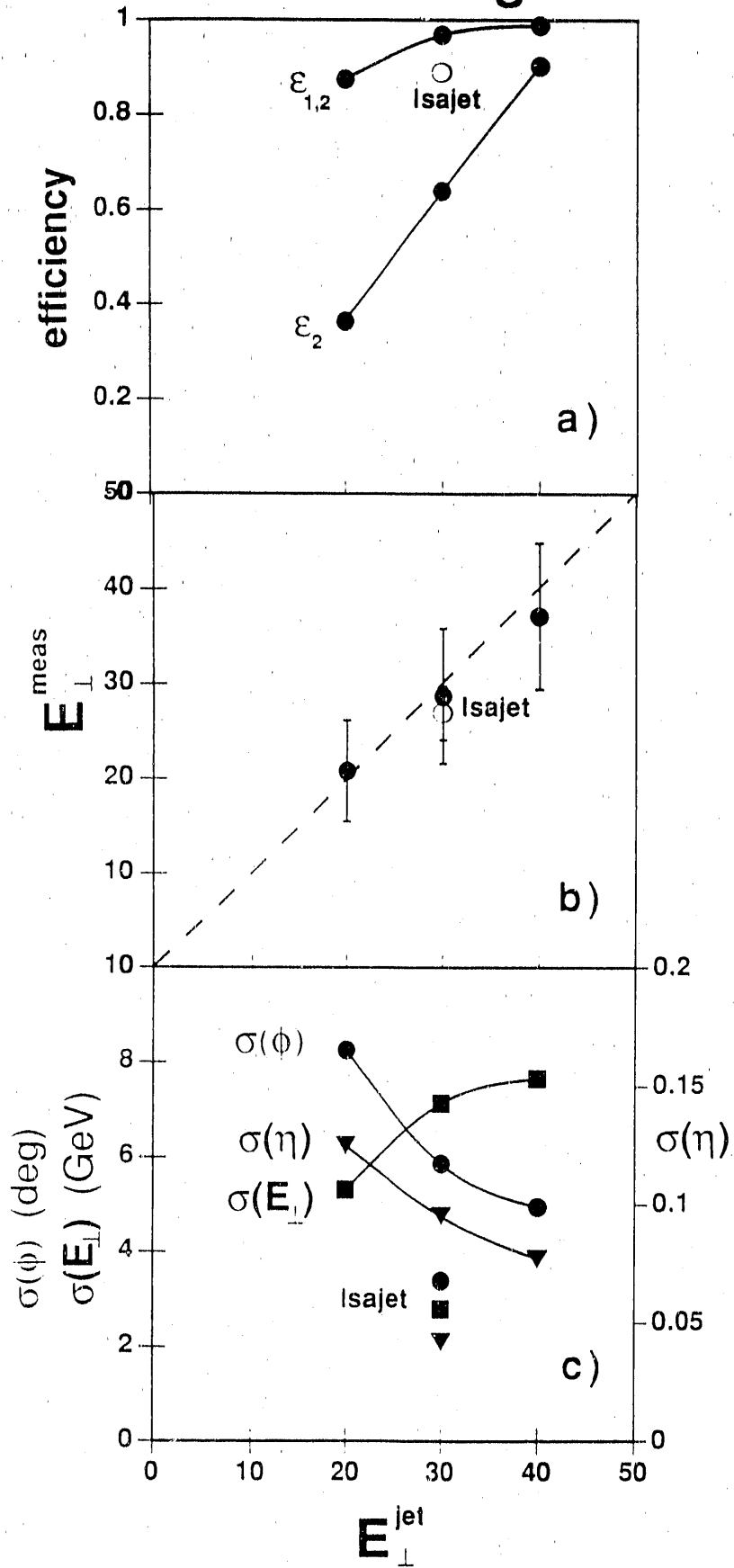


Fig. 4

# RHIC Experiment on Particle and Jet Production

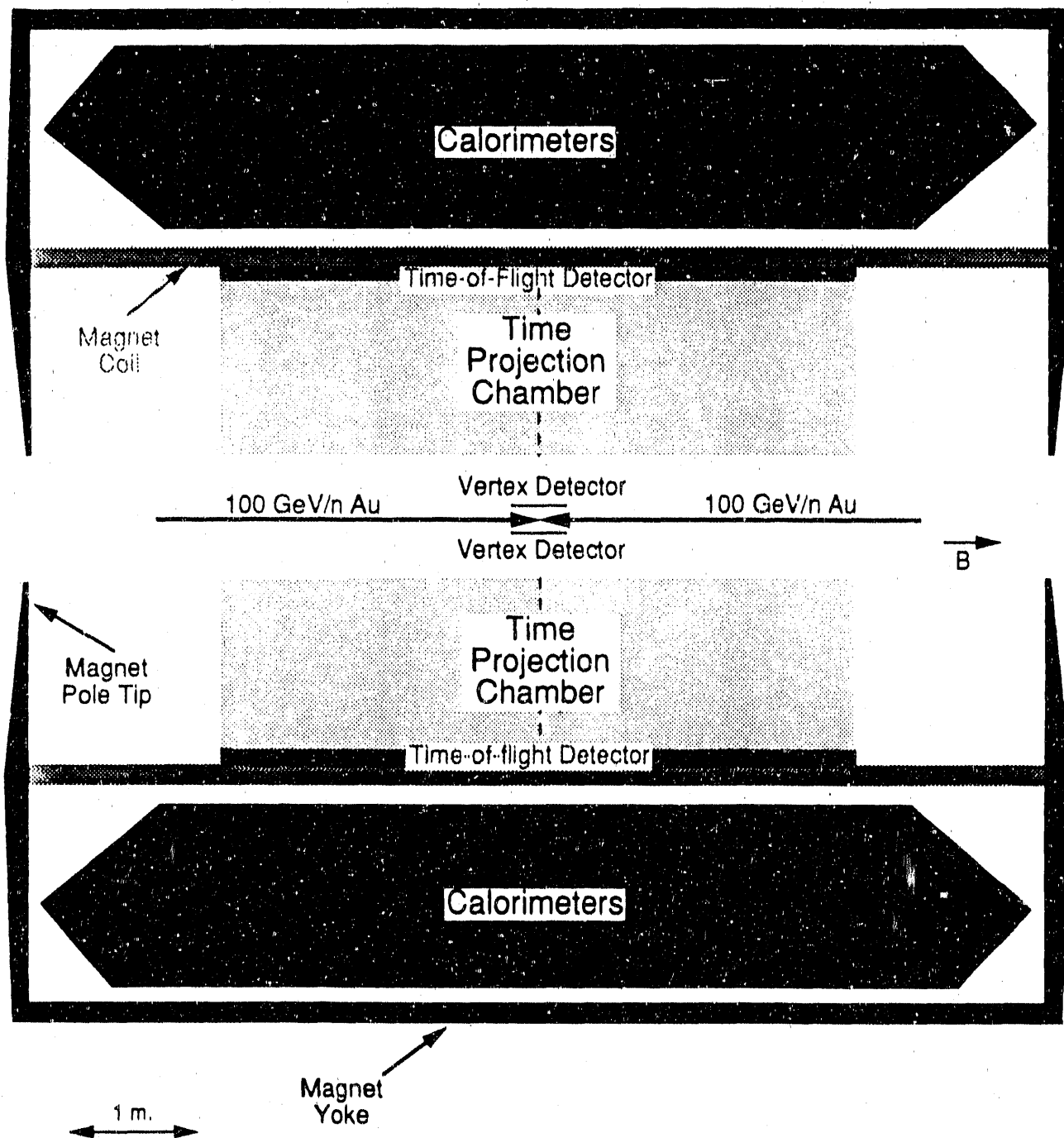


Fig. 5

### Momentum Resolution

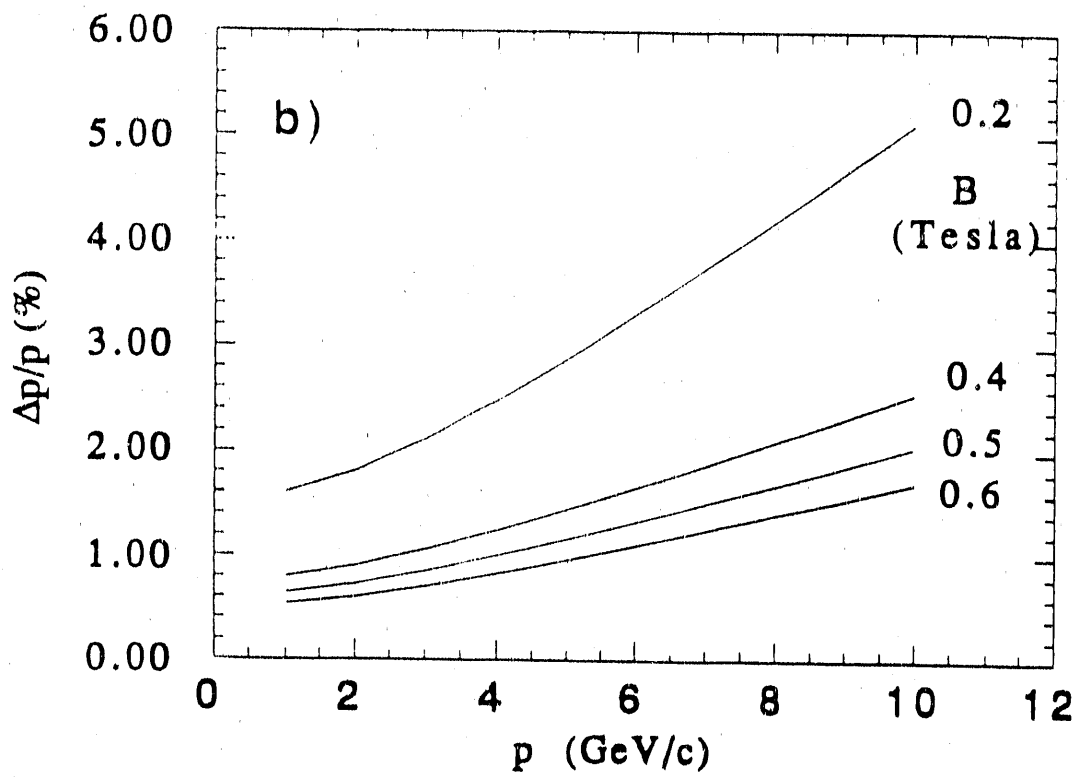
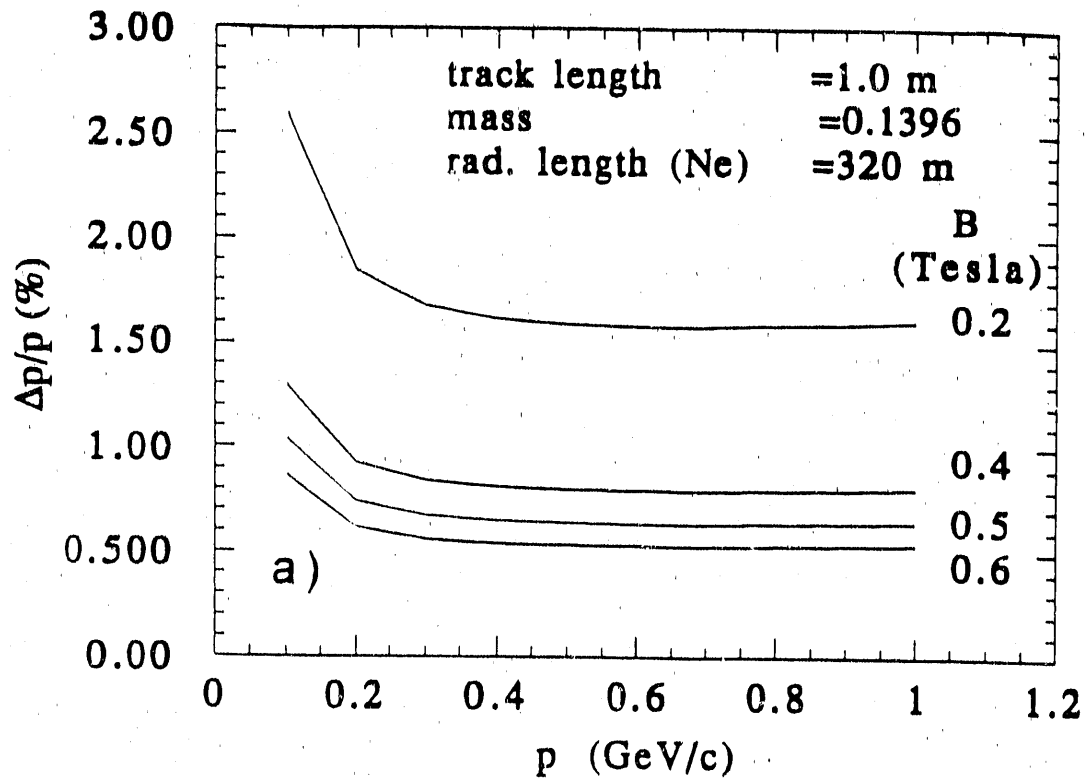


Fig. 6

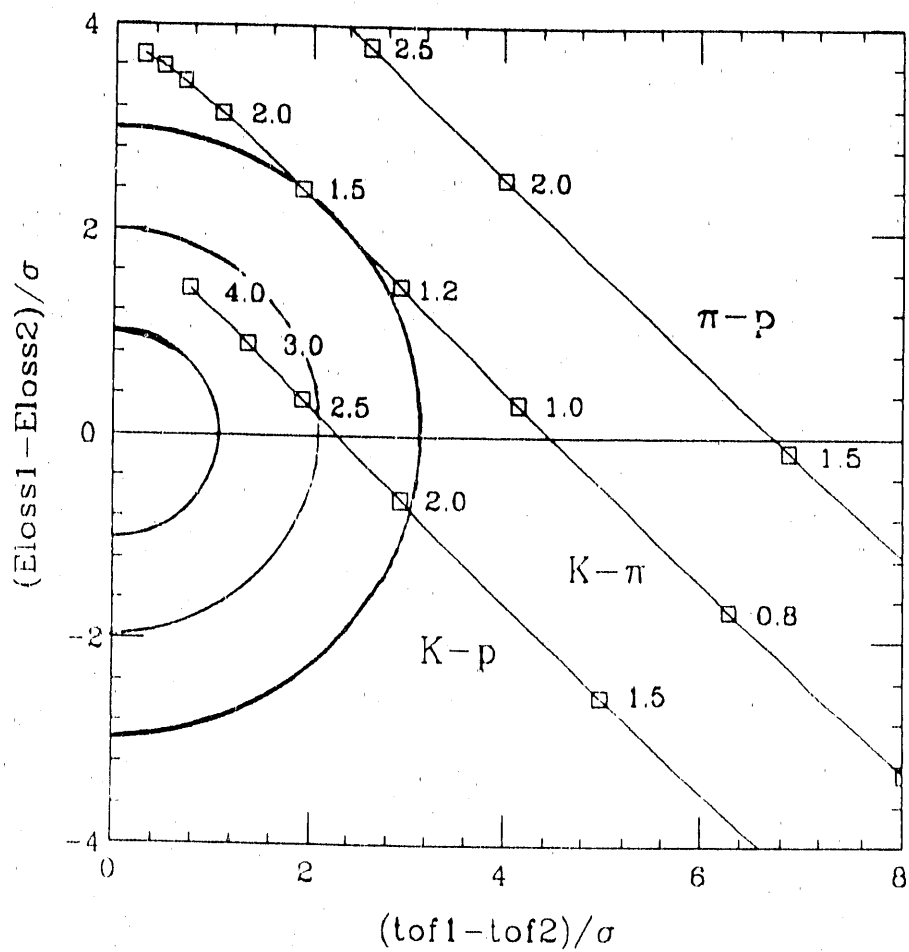


Fig. 7

**END**

**DATE FILMED**

10 / 24 / 90

